

Extracting 3D from Motion: Differences in Human and Monkey Intraparietal Cortex

W. Vanduffel,^{1,2*†} D. Fize,^{1*} H. Peuskens,^{1*} K. Denys,¹
S. Sunaert,³ J. T. Todd,⁴ G. A. Orban¹

We compared three-dimensional structure-from-motion (3D-SFM) processing in awake monkeys and humans using functional magnetic resonance imaging. Occipital and midlevel extrastriate visual areas showed similar activation by 3D-SFM stimuli in both species. In contrast, intraparietal areas showed significant 3D-SFM activation in humans but not in monkeys. This suggests that human intraparietal cortex contains visuospatial processing areas that are not present in monkeys.

To reconstruct the third dimension from a two-dimensional (2D) retinal image, our brain uses binocular as well as monocular cues such as shading, texture, and occlusion. Both humans and monkeys are also able to extract the 3D structure of an object from motion parallax cues that activate occipitoparietal areas in both species (1–3). Because neurons in the middle temporal area (MT/V5) are sensitive for speed gradients that reflect planes tilted in depth (4, see also 5), this area might play a crucial role in the extraction of depth from motion. Supporting evidence has been gleaned from a functional magnetic resonance imaging (fMRI) study showing 3D-SFM sensitivity in the human MT/V5 complex (hMT/V5+) (6). These human fMRI results raise a first question: To what extent can they be generalized to the primate visual system? Furthermore, anatomical evidence suggests that there might be functional differences between human and monkey intraparietal cortex: The intraparietal sulcus separates area 5 from area 7 in the monkey, whereas in humans these two areas belong to the superior parietal lobe. In addition, in humans, the intraparietal lobe separates area 7 from areas 39 and 40, which have no clear counterpart in monkeys (7). Therefore, our second goal was to determine whether monkey intraparietal cortex is as important for motion-dependent depth processing as implied by human imaging (6).

To address these issues, we turned to recently developed fMRI techniques (8) in awake (9–12) rather than anesthetized (13–14) monkeys. By performing human fMRI with virtually identical experimental procedures as in the awake monkey fMRI experiments, reliable interspecies comparisons could be made.

The stimuli were displays of nine randomly connected lines, rotating in depth, that created a clear 3D percept (movie S1). Control stimuli consisted of the same displays that were either static or moving in

one plane. We controlled for potential attentional differences between the 3D and 2D conditions by using a 1-back task in humans, as well as a demanding high-accuracy fixation task (8, 9) in both species.

In line with earlier reports (4–6, 13), area MT/V5 was activated more by 3D than by 2D moving random-line displays. In addition, the area in the fundus of the superior temporal sulcus (FST) also exhibited significant 3D-SFM sensitivity (Fig. 1A). Figure 2A shows the (3D – 2D) pattern of activation for a single human subject, and the average activation for a group of eight subjects is shown in Fig. 2B. These results are similar to those obtained in an earlier study in which somewhat different stimuli were used (6). Moreover, results from the motion-localizer scan indicated that 3D-SFM sensitivity occupies the most caudoventral part of the hMT/V5+ complex, suggesting that human FST is engaged in 3D-SFM processing.

Because motion is a monocular depth cue, our primary test stimuli were always presented monocularly. However, control tests revealed reproducible 3D-SFM sensitivity in macaque MT/V5 (and FST, figs. S1 and S2) and hMT/V5+, irrespective of whether the stimuli were presented monocularly or binocularly (fig. S2). Other control tests also revealed 3D-SFM sensitivity in macaque MT/V5 when random dot stimuli were used

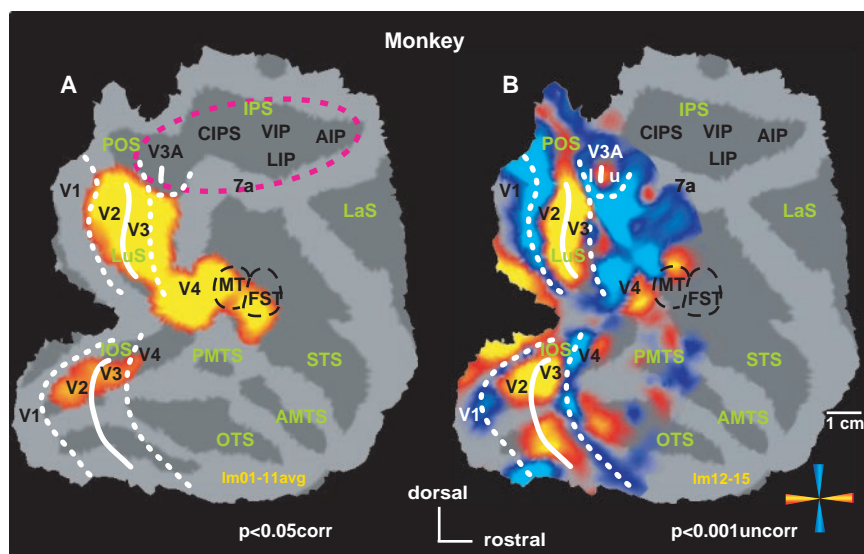


Fig. 1. 3D-SFM sensitivity in the monkey. (A) Statistical parametric map (t scores) for the subtraction (3D – 2D) overlaying the flattened right hemisphere of monkey M4 ($P < 0.05$, corrected for multiple comparisons). (B) Two overlaid t -score maps for the representation of the vertical (blue) and horizontal (yellow) meridians of the same hemisphere. The vertical and horizontal meridians are indicated by the dotted and straight white lines, respectively. A motion-localizer scan was used to define MT/V5 and FST (black dotted line). The purple outline indicates V3A and the intraparietal sulcus. Lowering the threshold to $P < 0.001$ (uncorrected for multiple comparisons) in the subtraction (3D – 2D) revealed only a few active voxels in VIP (fig. S1). AIP, anterior intraparietal area; AMTS, anterior middle temporal sulcus; CIPS, caudal intraparietal sulcus; IOS, inferior occipital sulcus; IPS, intraparietal sulcus; l, lower visual field representation; LaS, lateral sulcus; LIP, lateral intraparietal area; LuS, lunete sulcus; MT, middle temporal area; OTS, occipitotemporal sulcus; PMTS, posterior middle temporal sulcus; POS, parieto-occipital sulcus; STS, superior temporal sulcus; u, upper visual field representation.

¹Laboratorium voor Neuro- en Psychofysiologie, Katholieke Universiteit Leuven, Campus Gasthuisberg, Herestraat 49, Leuven B-3000, Belgium. ²MGH/MIT/HMS Athinoula A. Martinos Center for Biomedical Imaging, 13th Street, Building 149, Charlestown, MA 02129, USA. ³Afdeling Radiologie, UZ Gasthuisberg, Leuven B-3000, Belgium. ⁴Department of Psychology, Ohio State University, Columbus, OH 43210, USA.

*These authors contributed equally to this work.

†To whom correspondence should be addressed. E-mail: wim@nmr.mgh.harvard.edu or wim.vanduffel@med.kulcuven.ac.be

REPORTS

and when blood oxygen level–dependent (BOLD) fMRI signals were measured instead of monocrystalline ion oxide nanoparticle (MION) fMRI signals (8, fig. S2).

Regions within the lunate and inferior occipital sulcus exhibited significant 3D-SFM sensitivity (Fig. 1A and fig. S1). A retinotopic mapping experiment in the same subjects indicated that these activations correspond to areas V2 and V3 (Fig. 1B). These latter results fit with the observation in the anesthetized monkey [(13), but see supplementary online text] and with the present human fMRI experiment that revealed 3D-SFM sensitivity in retinotopically defined areas V2 and V3 (Fig. 2).

Monkey area V4, which can exhibit motion sensitivity under certain conditions (9, 15), also showed 3D-SFM sensitivity (Fig. 1A and fig. S1). This finding contrasts with the fMRI data from anesthetized monkeys, which show no 3D-SFM sensitivity to random dot stimuli in V4 (13). Yet our human fMRI results matched the awake monkey fMRI data: A large region of cortex immediately posterior to hMT/V5+ was more activated during 3D than during 2D moving displays. Previous human fMRI studies referred to this area as the lateral occipital sulcus (LOS) (6), the lateral occipital central/lateral occipital peripheral area (16), or as part of the lateral occipital complex (17–18). Similarity in functional properties (19), and in location with respect to V3A and MT/V5, between this human 3D-SFM–sensitive area and monkey area V4 favors the idea that the human region might correspond to area V4, as suggested earlier (19, 20).

In line with electrophysiological data, our previous monkey fMRI study (9) revealed no motion sensitivity in area V3A, unlike in human area V3A (supporting online text). A similar discrepancy between retinotopically defined human and monkey V3A was observed for 3D-SFM sensitivity (Figs. 1A and 2; fig. S1). Other cortical regions showing marked functional interspecies differences for 3D-SFM sensitivity were located in the intraparietal sulcus. In humans, four distinct intraparietal areas were engaged in the processing of 3D-SFM: the ventral intraparietal sulcus (VIPs), the parieto-occipital intraparietal sulcus (POIPS), the medial dorsal intraparietal sulcus (DIPSM), and the anterior dorsal intraparietal sulcus (DIPSA) (Fig. 2) (6). Despite strong motion-sensitivity for random line stimuli in the monkey's intraparietal sulcus (9) and the fMRI observations in anesthetized monkeys (13), we did not observe 3D-SFM sensitivity at a statistical threshold of $P < 0.05$, corrected for multiple comparisons (Fig. 2A), unless random dot stimuli were presented (fig. S2). Only very few voxels within the ventral intraparietal area (VIP) reached significance levels of $P < 0.001$, uncorrected for multiple comparisons (Fig. 3C and fig. S1). Such weak activation was also observed

in the anterior inferotemporal cortex (fig. S1).

It could be argued that the 3D moving stimuli are more interesting to observers than their 2D counterparts or that humans covertly attend to 3D stimuli more than monkeys do. Functional interspecies differences might thus be biased toward regions strongly modulated by attention, such as the intraparietal cortex (21). To control for possible differences in attention, we scanned three human sub-

jects while they performed a 1-back task that equalized and drew attention toward the 3D and 2D moving stimuli. Furthermore, monkey M1 and two human subjects were scanned while performing a demanding high-acuity fixation task (8, 9) that equalized but drew attention away from the stimuli presented in the background (22). The human subjects reached performance levels on the fixation task ($88 \pm 2\%$ correct) close to those of

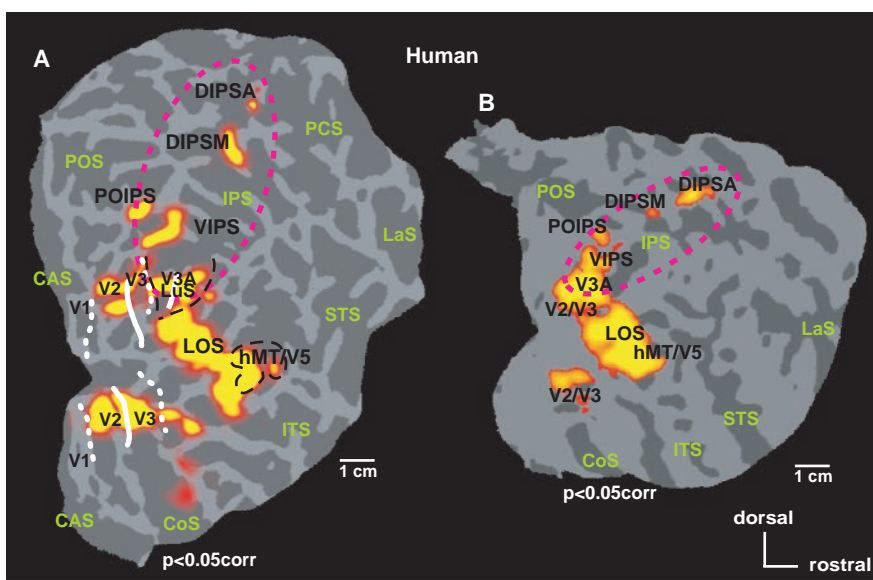


Fig. 2. 3D-SFM sensitivity in the human. The *t*-score maps (3D – 2D) of the right hemisphere of (A) one and (B) the average of eight human subjects (on an average anatomical reconstruction) are shown. The same conventions as in Fig. 1 are used to indicate the borders of the retinotopic and motion-sensitive areas (as revealed in separate scan sessions). The purple outline indicates V3A and the intraparietal sulcus. CAS, calcarine sulcus; CoS, collateral sulcus; ITS, inferotemporal sulcus; PCS, precentral sulcus.

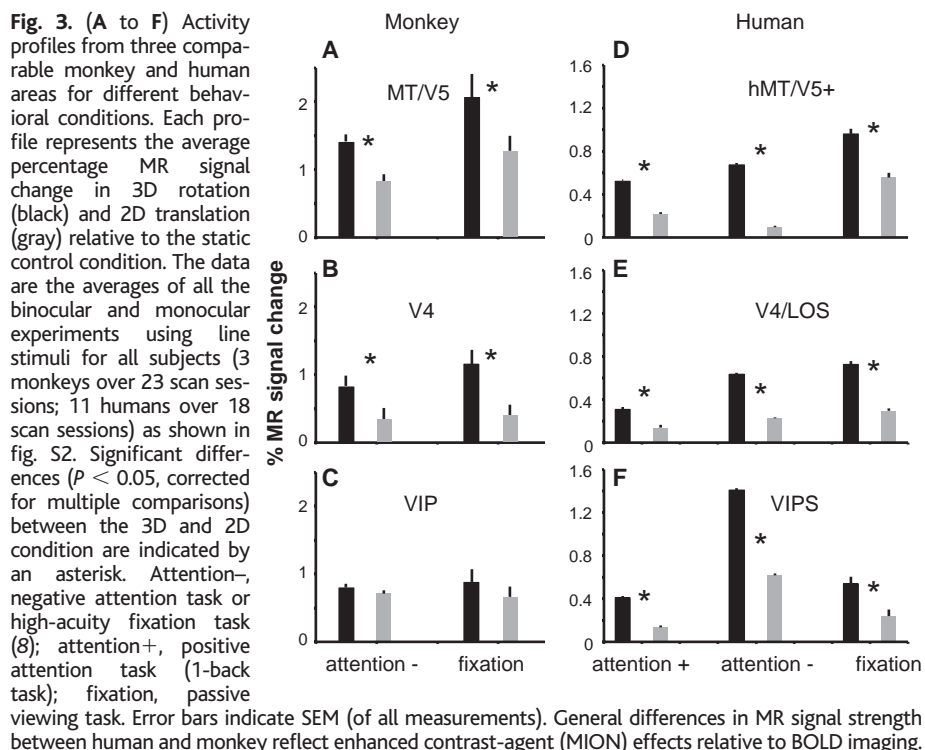


Fig. 3. (A to F) Activity profiles from three comparable monkey and human areas for different behavioral conditions. Each profile represents the average percentage MR signal change in 3D rotation (black) and 2D translation (gray) relative to the static control condition. The data are the averages of all the binocular and monocular experiments using line stimuli for all subjects (3 monkeys over 23 scan sessions; 11 humans over 18 scan sessions) as shown in fig. S2. Significant differences ($P < 0.05$, corrected for multiple comparisons) between the 3D and 2D condition are indicated by an asterisk. Attention–, negative attention task or high-acuity fixation task (8); attention+, positive attention task (1-back task); fixation, passive viewing task. Error bars indicate SEM (of all measurements). General differences in MR signal strength between human and monkey reflect enhanced contrast-agent (MION) effects relative to BOLD imaging.

REPORTS

monkey M1 ($96 \pm 5\%$ correct). Moreover, human subjects reported that they could not attend to the stimuli in the background of the fixation bar. Both these positive and negative attentional control tests yielded very similar activity patterns in the two species as obtained during the standard 3D-SFM tests (see “attention+” and “attention-” in Fig. 3). Furthermore, drawing attention away from the stimuli increased the difference between the 3D and 2D conditions within VIPS as compared with the passive viewing and the 1-back task conditions (Fig. 3F). These results indicate that the functional interspecies differences observed under passive viewing conditions are unlikely to reflect differences in attention between humans and monkeys.

Finally, to control for differences in second-order stimulus features such as spatial variations in speed, line length, and orientation changes over time (8) (table S1), we presented slowly rotating 3D displays, as well as in-plane rotating and expanding and contracting 2D displays. In most 3D-SFM-sensitive brain regions in monkeys and humans as described above, the two main 3D stimuli (original and slow) yielded statistically higher activity levels as compared with the three 2D control stimuli (Fig. 4). The main exceptions were in the early retinotopic regions (V2, V3, and hV3A) and FST, where 2D rotation or expansion and contraction yielded MR signals that were statistically indistinguishable from those of the 3D displays (supporting online text).

In this study, we compared the neuronal

substrate involved in the processing of 3D-SFM in awake human and nonhuman primates. The two species share a network of early and midlevel visual areas (V2, V3, V4, MT/V5, and FST) with similar sensitivity for 3D-SFM. These areas in monkeys and humans could be identified independently by using the combination of retinotopic mapping and motion-sensitivity tests. At least for V4 and MT/V5, and their presumptive human homologs, multiple control experiments demonstrated the specificity of this activation (Fig. 4). Pronounced functional differences between the two species were observed in V3A and the intraparietal cortex, which are unlikely to reflect attentional factors. The widespread human intraparietal 3D-SFM sensitivity might indicate the existence of an additional motion pathway in the human, projecting from V3A to the intraparietal sulcus. Although differences between human and monkey parietal cortex have been suggested (23–25), direct functional comparisons could not be conducted. The sole direct comparisons published to date reported only similarities between human and monkey prefrontal cortex (10). The present results suggest that, under evolutionary pressure, parietal but not earlier regions adapted to implement human-specific abilities such as excellent motion-dependent 3D vision for manipulating fine tools (supporting online text). This adaptation could involve displacement of homologous regions (25). Alternatively, new posterior parietal areas could have been evolved before the enormous frontal enlargement in recent

hominid development. The latter mechanism has been suggested for areas 39 and 40 (7). Finally, the present results call for follow-up studies investigating whether similar functional dissimilarities in the intraparietal sulcus exist for the processing of other 3D cues such as disparity (supporting online text) and the extent to which the intraparietal species differences in 3D-SFM processing are related to behavioral performance.

References and Notes

1. S. Ullmann, *The Interpretation of Visual Motion* (MIT Press, Cambridge, MA, 1979).
2. J. T. Todd, in *High-Level Motion Processing*, T. Watanabe, Ed. (MIT Press, Cambridge, MA, 1998), pp. 359–377.
3. R. M. Siegel, R. A. Andersen, *Nature* **331**, 259 (1988).
4. D. K. Xiao, V. L. Marcar, S. E. Raiguel, G. A. Orban, *Eur. J. Neurosci.* **9**, 956 (1997).
5. D. C. Bradley, G. C. Chang, R. A. Andersen, *Nature* **392**, 714 (1998).
6. G. A. Orban, S. Sanaert, J. T. Todd, P. Van Hecke, G. Marchal, *Neuron* **24**, 929 (1999).
7. H.-O. Karnath, *Nature Rev. Neurosci.* **2**, 568 (2001).
8. Materials and methods are available as supporting material on Science Online.
9. W. Vanduffel et al., *Neuron* **32**, 565 (2001).
10. K. Nakahara, T. Hayashi, S. Konishi, Y. Miyashita, *Science* **295**, 1532 (2002).
11. D. J. Dubowitz et al., *Neuroreport* **9**, 2213 (1998).
12. L. Stefanacci et al., *Neuron* **20**, 1051 (1998).
13. M. E. Sereno, T. Trinath, M. Augath, N. K. Logothetis, *Neuron* **33**, 635 (2002).
14. N. K. Logothetis, J. Pauls, M. Augath, T. Trinath, A. Oeltermann, *Nature* **412**, 150 (2001).
15. A. S. Tolias, S. M. Smirnakis, M. Augath, T. Trinath, N. K. Logothetis, *J. Neurosci.* **21**, 8594 (2001).
16. R. B. H. Tootell, A. M. Dale, M. I. Sereno, R. Malach, *Trends Neurosci.* **19**, 481 (1996).
17. R. Malach et al., *Proc. Natl. Acad. Sci. U.S.A.* **92**, 8135 (1995).
18. K. Grill-Spector, Z. Kourtzi, N. Kanwisher, *Vision Res.* **41**, 1409 (2001).
19. K. Nelissen et al., paper presented at the 30th Annual Meeting of the Society for Neuroscience, New Orleans, LA, 4 November 2000.
20. R. B. H. Tootell, N. Hadjikhani, *Cereb. Cortex* **11**, 298 (2001).
21. E. P. Cook, J. H. R. Maunsell, *J. Neurosci.* **22**, 1994 (2002).
22. A. C. Huk, D. Ress, D. J. Heeger, *Neuron* **32**, 161 (2001).
23. D. Eidelberg, A. M. Galubardi, *Arch. Neurol.* **41**, 843 (1984).
24. A. D. Milner, in *Parietal Lobe Contributions to Orientation in 3D Space*, P. Thier, H.-O. Karnath, Eds. (Springer Verlag, Heidelberg, Germany, 1997), pp. 843–852.
25. O. Simon, J.-F. Mangin, L. Cohen, D. Le Bihan, S. Dehaene, *Neuron* **33**, 475 (2002).
26. We are grateful to K. Nelissen for helping in the initial pilot studies. We thank Y. Celis, A. Coeman, M. De Paep, W. Depuydt, C. Franssen, P. Kayenberg, G. Meulemans, and G. Vanparijs for technical support. W.V. and H.P. are research fellows of FWO-Flanders. Supported by grants GSKE, FWO G0112.00, GOA 2000/11, IUAP 5/10, and MAPAWAMO (EU, Life Sciences Project).

Supporting Online Material

www.sciencemag.org/cgi/content/full/298/5592/413/DC1

Materials and Methods

Supporting Text

Figs. S1 and S2

Table S1

References and Notes

Movie S1

3 May 2002; accepted 8 August 2002

Fig. 4. (A and B) Control for potential differences in higher-level stimulus characteristics in 3D-SFM-sensitive regions. Activity profiles represent the average percentage signal change of the two hemispheres relative to the static control condition (from eight sessions in monkeys M3 and M4 and six sessions in three human subjects). Error bars indicate SEM. Changes in line orientation and line length, as well as spatial variations of the speed of the lines, do not explain the observed 3D-sensitivity in MT/V5 and V4 and their presumptive human homologs.

